scientific reports

Check for updates

OPEN

SPG601-associated modulation of resting-state EEG and improvement in executive function in a fragile X syndrome randomized controlled crossover study

Ernest V. Pedapati[1,2,3], Peter W. Vanderklish[4], Stella T. Sarraf[4], Sharron Gargosky[4], Meredith Nelson[5,6], Sarah Richter[1], Grace Westerkamp[1] & Craig A. Erickson[1,3]✉

Fragile X syndrome (FXS) is the most common inherited cause of intellectual disability and autism spectrum disorder. Despite extensive research, no targeted treatments exist for the core symptoms of FXS. SPG601 represents the first BK channel activator to enter clinical testing for FXS, designed to restore synaptic function by correcting specific ion channel dysfunction downstream of fragile X messenger ribonucleoprotein protein (FMRP) loss. We conducted a randomized, double-blind, placebo-controlled, 2-period balanced crossover study in 10 adult men with genetically confirmed full-mutation fragile X syndrome. Participants received single doses of SPG601 800 mg and placebo separated by a 1-week washout period. Given the first in FXS nature of the study, the safety and tolerability of SPG601 were evaluated as a primary outcome. Additional endpoints included resting-state EEG power spectral density analysis across predefined frequency bands and auditory-evoked gamma oscillations combined with cognitive assessments using validated instruments and clinical global impressions scales. Among EEG measurements, excessive high frequency gamma band activity has been most extensively validated as a biomarker across species in FXS and has demonstrated correlation with severity of the human FXS phenotype and therefore served as the primary neurophysiologic endpoint. SPG601 was well tolerated with a favorable safety profile. SPG601 demonstrated significant modulation of resting-state EEG power spectral density compared to placebo. Significant treatment effects were observed for gamma power ($F = 5.20$, $p = 0.023$), alpha2 power ($F = 17.43$, $p < 0.001$), and theta power ($F = 7.06$, $p = 0.008$). SPG601 also significantly modulated aperiodic EEG slope ($F = 5.28$, $p = 0.022$), indicating alterations in the broadband 1/f component reflecting excitation-inhibition balance. Cognitive improvement was observed in the NIH Toolbox Flanker Inhibitory Control and Attention Test across multiple scoring metrics ($p = 0.027$). No significant effects were observed on auditory-evoked gamma measures. This study provides the first clinical evidence that SPG601 produces significant neurophysiological changes in FXS, accompanied by a cognitive enhancement in executive function.

Keywords Fragile X syndrome, BK channels, EEG biomarkers, Neurophysiology, Cognitive function, Clinical trial

Fragile X syndrome (FXS) is the most common inherited form of intellectual disability and autism impacting 1 in 4,000 individuals globally[1,2]. As an X linked disorder, FXS significantly impacts all affected males and on average half of females showing significant clinical symptoms. The identification of phenotypically relevant and

[1]Division of Child and Adolescent Psychiatry, Cincinnati Children's Hospital Medical Center, 3333 Burnet Ave, Cincinnati, OH 45229-3039, USA. [2]Division of Neurology, Cincinnati Children's Hospital Medical Center, 3333 Burnet Ave, Cincinnati, OH 45229-3039, USA. [3]Department of Psychiatry and Behavioral Neuroscience, University of Cincinnati College of Medicine, Stetson Building Suite 3200, 260 Stetson Street, Cincinnati, OH 45267-0559, USA. [4]Spinogenix Inc, 1801 Century Park East,Suite 2400, Los Angeles, CA 90067, USA. [5]Division of Behavioral Medicine and Clinical Psychology, Cincinnati Children's Hospital Medical Center, 3333 Burnet Ave, Cincinnati, OH 45229-3039, USA. [6]Department of Pediatrics, University of Cincinnati College of Medicine, 3333 Burnet Ave, Cincinnati, OH 45229-3039, USA. ✉email: craig.erickson@cchmc.org

pharmacologically viable therapeutic targets has been challenging[3] in large part due to the pleiotropic nature of FMRP function as an RNA-binding protein that exerts broad and complex regulatory effects on the proteome, primarily through translational regulation[4,5].

It is now appreciated that FMRP also plays a critical role as a positive modulator of several potassium channels that sculpt the activity of synaptic circuits involved in FXS symptomology[6–9]. Among these, particularly strong support has emerged that reductions in the activity of large conductance, Ca^{++}-activated potassium channels (BK channels) are etiologically relevant to FXS symptomology (please see Supplemental Materials for an in-depth description of BK channels).

A broad set of complementary findings at the molecular, electrophysiological, genetic and behavioral levels provide strong support for the hypothesis that positive modulation of BK channels may be an effective therapeutic approach in FXS. At a molecular level, there is evidence that FXS impairs BK channel activity in two ways. Early studies of the synaptic proteome in FXS revealed that Kcnma1a protein expression is reduced by ~ 50%[10]. Taken with prior reports on haploinsufficiency of the Kcnma1a gene in individuals with autism and intellectual disability[11], this suggested that impaired translation of Kcnma1a mRNA, an FMRP target[4], in FXS may mimic haploinsufficiency in contributing to autism and ID symptoms. It was later discovered that translation-independent effects of FMRP loss impair BK channel function in FXS. FMRP is a positive modulator of BK channels, increasing the Ca^{++} sensitivity and altering the gating kinetics of BK channels through direct associations with b4 subunits[12,13] and a1 subunits[6]; the more prominent effect is seen for b4-containing channels[13,14]. Accordingly, studies in *Fmr1* KO mice have demonstrated an increase in action potential broadening during high frequency transmission, along with increases in glutamate release[12–15] and seizure susceptibility[13]. Genetic upregulation of BK channel activity by deletion of the b4 subunit rescued these synaptic and circuit phenotypes[13]. Further highlighting the importance of the b4 subunit, a mutation in FMRP (R138Q) associated with intellectual disability that blocks its association with the b4 subunit, while sparing its translational regulatory activity, results in channel hypoactivity and attendant action potential broadening[14]. Pharmacological rescue of synaptic and behavioral phenotypes of the *Fmr1* KO mouse has been demonstrated using BMS-204,352, a clinical stage BK channel opener originally developed for stroke that failed to meet endpoints and was not suitable for clinical development in chronic indications such as FXS due to oral bioavailability limitations[16].

The potential for BK channel positive modulation to correct circuit level activity changes may be particularly important in FXS insofar as increased cortical excitability has been linked to sensory hypersensitivity and other symptoms[17,18]. BK channel modulation may induce acute and potentially chronic effects neuronal circuit dynamic effects via BK-NMDA channel coupling[19,20] impacting neuronal burst firing and neurotransmitter release. Of particular potential importance, BK-NMDA coupling dynamics have been implicated more broadly in the pathophysiology of autism spectrum disorder (ASD)[21], a neurodevelopmental condition significantly overlapping with FXS.

Augmenting BK channel activity by knockdown of the b4 subunit in *Fmr1* KO mice rescued synaptic integration defects in layer V pyramidal cells that may play a role in sensory symptoms of FXS[22]. In addition, the BK channel positive modulator BMS-204,352 rescued cortical circuit abnormalities and sensory hypersensitivity in the *Fmr1* KO mouse that are thought to be related to sensory hypersensitivity in FXS[23,24]. A related BK positive modular, BMS-191,011, was found to rescue cortical dendrite hyperexcitability[24]. Cortical hyperexcitability phenotypes are evident in FXS patients, particularly in males, who consistently exhibit increased gamma frequency band power (30–70 Hz) during resting-state EEG, with specific neocortical localization and disrupted thalamocortical modulation that correlates with intellectual disability severity[18,25]. Recent machine learning approaches have demonstrated that EEG measures can reliably discriminate individuals with FXS from typically developing controls, with resting frontal theta power and chirp-evoked oscillatory responses showing particularly robust discriminative power[26]. The electrophysiological alterations extend beyond gamma band abnormalities to include altered EEG microstates, which serve as markers for cognitive impairments and attention deficits characteristic of FXS[27].

Importantly, EEG biomarkers show high test-retest reliability in FXS populations and strong translational validity, with neurophysiological abnormalities conserved across human patients and Fmr1 knockout mouse models[28]. This reliability and the phenotypic relevance of EEG as an objective and quantitative translational outcome measure may help address limitations of current translational approaches. To date, clinically-tested mechanisms of action have failed to normalize established EEG phenotypes in preclinical and clinical models[29,30], illustrating the translational importance of modulating brain activity patterns and emphasizing the need for novel therapeutic targets including BK channel positive modulators that can in principle normalize network level activity defects in FXS. Overall, we postulate that BK channel hypofunction in FXS is a significant driver of cortical hyperexcitability and symptoms in FXS, and that BK channel positive modulation may show efficacy at both the behavioral and neurophysiological levels. Cortical hyperexcitability is demonstrated by resting EEG abnormalities in FXS including elevated gamma, altered alpha and theta activity, and abnormal aperiodic slope. These resting EEG abnormalities are then associated with many of the clinical manifestations of FXS such as sensory hypersensitivity and executive dysfunction.

Prior preclinical and clinical studies with SPG601, a novel BK channel opener acting on the b4 subunit[31–33], support its suitability for clinical development in FXS as a treatment to offset deficits in BK channel activity. In preclinical work, SPG601 rescued a range of phenotypes in the *Fmr1* KO mouse, including: hyperactivity, memory, stereotypy and behaviors analogous to activities of daily living in humans[8]. SPG601 is CNS penetrant and exhibits high oral bioavailability in humans. Importantly, prior Phase 1 (EudraCT 2013–002765-18) and Phase 2 (spasticity related to multiple sclerosis; NCT02542787) clinical studies established that SPG601 has a very favorable safety and tolerability profile. In consideration of its drug-like properties, safety and tolerability profile, and unique MoA with the potential to reverse core deficits in synaptic and cortical function, we conducted a proof-of-concept Phase 2a clinical trial of SPG601 in adult males with FXS.

Here we report results from a randomized, double-blind, placebo-controlled crossover study of single-dose SPG601 in adult men with FXS. Same day assessments were performed before drug administration and again at the Tmax of ~2 h. The study design addresses critical gaps in FXS drug development by employing objective neurophysiological measures that bridge preclinical findings with clinical outcomes. This approach leverages the demonstrated reliability and discriminative power of EEG biomarkers in FXS populations, utilizing validated measures that can reliably distinguish individuals with FXS from controls with high accuracy[26]. The comprehensive neurophysiological assessment included both resting-state power spectral analysis and auditory-evoked responses, complemented by standardized performance-based assessments to evaluate functional outcomes. By focusing on BK channel modulation through SPG601, this study represents a paradigm shift toward targeting proximal molecular consequences of FMRP loss rather than downstream pathways, potentially overcoming the translational challenges that have limited previous therapeutic approaches in this field[30,34].

Methods

Study design and participants

This phase 2a study employed a randomized, double-blind, placebo-controlled, 2-period balanced crossover design to evaluate the neurophysiological effects of single-dose SPG601 in ten 18–45 year old men with FXS defined by Southern Blot and PCR testing consistent with > 200 CGG repeats in the FMR1 without any evidence of repeat size or methylation mosaicism. Key exclusion criteria included concurrent use of investigational agents, significant medical comorbidities that could interfere with study assessments, and inability to tolerate EEG procedures. A total of 10 participants were enrolled and randomized in a 1:1 ratio to receive either SPG601 800 mg followed by placebo, or placebo followed by SPG601 800 mg, with a 1-week washout period between treatments (± 2 days; please see Supplemental Figure Flow Chart of Experimental Paradigm The 7-day washout was chosen to exceed > 5 half-lives of the drug by a wide margin based on prior pK studies with SPG601 while at the same time creating a study visit schedule that was stakeholder friendly (versus for example 2 visits in 3–4 days). The crossover design was selected to optimize statistical power while minimizing interindividual variability, a well-established approach for clinical trials in populations with high phenotypic heterogeneity. The study was conducted at Cincinnati Children's Hospital Medical Center between July 2024 and November 2024, with approval from the institutional review board and written informed consent obtained from all participants and their legally authorized representatives.

Randomization and blinding

Participants were randomly assigned using a computer-generated randomization schedule to one of two treatment sequences. Randomization was balanced to ensure equal allocation to each sequence arm. Study drug and placebo were identical in appearance and packaging to maintain blinding. Participants, caregivers, investigators, and all study personnel remained blinded to treatment assignment throughout the study period and data analysis phase.

Study procedures and assessments

All study visits were conducted in a standardized clinical research environment. Participants were administered study medication in the fed state, consistent with routine clinical practice, after consuming a standardized breakfast. The timing of assessments was based on SPG601 pharmacokinetic data showing peak plasma concentrations at 2 h post-dose in the fed state, with a half-life of approximately 3–4 h.

Safety monitoring

Safety was assessed through adverse event monitoring, vital signs, clinical laboratory evaluations (hematology and clinical chemistry), 12-lead electrocardiography, physical examinations, and suicidality assessment using the Columbia Suicide Severity Rating Scale. All adverse events were coded using Medical Dictionary for Regulatory Activities (MeDRA) terminology and assessed for severity and relationship to study drug.

Neurophysiological EEG endpoints

Resting-state electroencephalography was performed 2 h post-dose using a high-density 128-channel system following established protocols for fragile X syndrome research (Wang et al., 2017; Lovelace et al., 2018). Participants were seated comfortably in a sound-attenuated room with eyes open during 5-minute recording epochs. EEG data were acquired at 1000 Hz sampling rate with impedances maintained below 50 kΩ. Data preprocessing included bandpass filtering (0.5–100 Hz), artifact rejection using automated and manual procedures, and source localization using standardized head models.

Power spectral density analysis focused on predefined frequency bands based on prior fragile X syndrome research: delta (1–4 Hz), theta (4–8 Hz), alpha1 (8–10 Hz), alpha2 (10–12 Hz), beta (12–30 Hz), gamma1 (30–50 Hz), and gamma2 (50–70 Hz)[25,35]. Statistical analysis employed linear mixed-effects models accounting for the crossover design, with treatment condition and brain region as fixed effects and participant as a random effect.

Clinical and cognitive assessments

Clinical outcomes were assessed using validated instruments immediately following EEG recording. The Clinical Global Impressions-Severity (CGI-S), and -Improvement (CGI-I) scales (Guy, 1976) were administered by trained clinicians and caregivers to provide a brief rating of overall symptom severity and improvement. The NIH Toolbox Cognition Battery (NIHTB-CB)[36] was utilized as the primary performance-based study measure of executive function and cognitive performance. The NIHTB-CB is a standardized, tablet-based brief measure of cognitive abilities that is validated for individuals aged 3–85 years). It includes Fluid Cognition and Crystalized Cognition domains. The Fluid Cognition domain is comprised of the following three subtests:

Flanker Inhibitory Control and Attention Test, Dimensional Change Card Sort Test, and the Pattern Comparison Processing Speed Test. The Crystalized Cognition domain is comprised of the Picture Vocabulary Test and Oral Reading Recognition Test. Additional subtests administered involved with Fluid Cognition and processing speed included the Flanker Inhibitory Control and Attention Test, Dimensional Change Card Sort Test, and the Pattern Comparison Processing Speed Test and Speeded Matching.

Subject molecular characterization

Subject peripheral blood fragile X messenger ribonucleoprotein (FMRP) levels were determined at baseline using immunoassay techniques established in FXS[37].

EEG Preprocessing.

EEG data were blindly preprocessed using an automated pipeline implemented in Python 3.13 (MNE-Python, PyLossless) using Brain Imaging Data Structure (BIDS) format to facilitating standardized data organization and analysis. Raw EEG data was acquired using 128-channel HydroCel Geodesic Sensor Net system (MAGSTIM/EGI) were imported into MNE-Python 1.9. For both the resting-state and chirp tasks, data were resampled to 250 Hz. Data were trimmed by four seconds from the beginning and end of each recording. *PyLossless Pipeline*: For advanced artifact reduction we employed the PyLossless pipeline. The core principle of PyLossless is its non-destructive approach, which prioritizes annotation of artifacts over irreversible data alteration, thereby preserving the integrity of the original EEG recordings and facilitating reproducible analyses. The pipeline begins with digital filtering, applying a band-pass filter between 1 and 100 Hz to mitigate slow drifts and high-frequency noise, and a 60 Hz notch filter to remove power line interference. Following filtering, a two-stage Independent Component Analysis (ICA) approach for robust artifact decomposition was performed. The first decomposition used (FASTICA) removes non-stationary data segments to improve the accuracy of the second ICA in classifying ICs based on their likely origin. Then extended infomax ICA algorithm was performed to decompose the EEG data into 64 independent components. Automatic classification of these components was achieved using mne-iclabel (0.7) to identify components related to artifacts such as muscle activity, cardiac signals, eye movements, and channel or line noise. Following automatic classification, ICA components flagged as artifacts (IC types: 'muscle', 'heart', 'eog', 'ch_noise', 'line_noise' with a confidence threshold of 0.3) were manually reviewed and subsequently removed from the data to enhance signal quality for downstream analysis. Next for resting-state task, fixed-width epochs were further cleaned based on global field power (GFP) values. Epochs exceeding a GFP z-score threshold of 3 were excluded. For the chirp task, continuous data were segmented into epochs time-locked to stimulus start, spanning from 0.5 s before to 2.7 s after the event onset. Quality control reports, including visualizations of ICA components, power spectral density (PSD) plots, topographical maps of band power, and plots of raw vs. cleaned data, were automatically generated as PDF and PNG files using custom functions within the pipeline.

Resting-state spectral power analysis

Resting-state spectral power was calculated on continuous EEG data using Welch's method, as implemented in the MATLAB *pwelch* function. This method estimates the power spectral density (PSD) by averaging modified periodograms of overlapping segments of the data. For each participant, we analyzed 80 s of continuous EEG data. The data were segmented using a Hanning window with a length of 2 s and an overlap of 50% between segments. The PSD was computed across a broad frequency range, from 1 Hz to 120 Hz, with a frequency resolution of 0.5 Hz. From the PSD, we derived absolute power (in V^2/Hz and dB/Hz) and relative power (unitless, normalized to total power). Furthermore, band-averaged power was calculated by averaging the PSD values within pre-defined frequency bands: delta (1–4 Hz), theta (4–8 Hz), alpha1 (8–10 Hz), alpha2 (10–12 Hz), beta (12–30 Hz), gamma1 (30–50 Hz), and gamma2 (50–70 Hz). These power calculations were performed channel-wise to obtain spectral power estimates for each electrode across the defined frequency bands.

EEG source estimation

To estimate neural sources underlying the scalp EEG data, we performed source localization using Brainstorm software. A forward model was computed using a three-layer boundary element method (BEM) based on OpenMEEG, employing the default ICBM152 anatomical template within Brainstorm and EGI 128-channel montage. The BEM model comprised compartments for scalp, skull, and brain, with default conductivity values within OpenMEEG. For the inverse solution, we implemented a Minimum Norm Estimate (MNE) with amplitude as the inverse measure, utilizing fixed source orientations constrained to the cortex and a loose orientation constraint of 0.2. Depth weighting was applied with an exponent of 0.5 and a weight limit of 10 to mitigate depth bias inherent in MNE. An identity matrix was used for noise covariance as recommended for continuous EEG data. A fixed Signal-to-Noise Ratio (SNR) method was used with an SNR value of 3 to determine the regularization parameter for the inverse solution. Source space was constrained to the cortex surface, and source activity was parcellated according to the Desikan-Killiany atlas, encompassing 68 cortical regions, with regional source time series extracted by averaging vertex activity within each scout (region). This allowed us to estimate source activity within anatomically defined brain regions for subsequent analyses.

Peak alpha frequency analysis

To quantify individual alpha peak frequency (IAF), we implemented an automated custom Python script based on the method described by Dickinson et al. (2018)[38]. This analysis was performed on pre-computed relative power spectral density (PSD) data, derived from resting-state EEG recordings. For each channel (F3, F4, C3, C4, O1, O2) and subsequently for frontal, central, and occipital regions (averaged across channels within each region), the power spectrum was analyzed within a frequency range of 6–12 Hz, encompassing the typical.

alpha band. The method involves several steps: first, the power spectrum is log-transformed, and a 1/f trend is removed using linear regression in log-log coordinates, followed by Savitzky-Golay filtering to smooth the detrended spectrum. Within the alpha frequency range (6–12 Hz), potential peaks are identified using a *scipy.signal.find_peaks*. The most prominent peak within the alpha range is then refined by fitting a Gaussian curve (*scipy.optimize.curve_fit*). The center frequency of the fitted Gaussian is taken as the IAF for the channel or region. If Gaussian fitting failed or no valid peak was identified within the alpha range by peak-finding, a fallback method selects the frequency with the maximum power within the 6–12 Hz range as the IAF. Thisprocess yielded peak alpha frequency values for each selected channel and region, which were then summarized and visualized, including topographical heatmaps and individual channel/region spectral plots (Fig. 1).

Aperiodic component parameterization with FOOOF

To characterize the aperiodic, or 1/f-like, background activity in the neural power spectra, we utilized the Fitting Oscillations & One Over F (FOOOF) algorithm, implementing a custom MATLAB function using the Brainstorm implementation. For each source localized region of interest, we modeled the aperiodic component of the power spectrum across a frequency range of 1–55 Hz. The aperiodic fitting was performed using the 'knee' model, which allows for a bend in the 1/f slope, thus capturing variations in the aperiodic component beyond a simple linear trend (Fig. 2). To enhance the robustness of the aperiodic fit against potential outliers in the power spectrum, a robust fitting procedure was employed within FOOOF. This involved an iterative approach to minimize the influence of outlier data points on the estimated aperiodic parameters, specifically the offset, exponent (slope), and knee frequency.

Inter-trial coherence and event-related spectral perturbation analysis

To examine phase-locked and non-phase-locked responses to the auditory chirp stimuli, we calculated inter-trial coherence (ITC) and event-related spectral perturbation (ERSP) measures. These time-frequency analyses were computed using the EEGLAB function *newtimef*, a legacy function we utilized for consistency with prior pipeline iterations. Time-frequency decompositions were performed on epoched EEG data, for frequencies ranging from 2 to 110 Hz, with frequency resolution determined by 109 frequency bins spaced linearly, and for a time window from − 500 ms to 2750 ms relative to stimulus onset. We used wavelet cycles varying from 1 cycle at the lowest frequency to 30 cycles at the highest frequency, and a window size of 100 data points for the wavelet convolution. To correct for potential inflation of ITC values due to trial count, we applied a critical value correction based on the number of trials. We calculated mean ITC and ERSP values within pre-defined time-

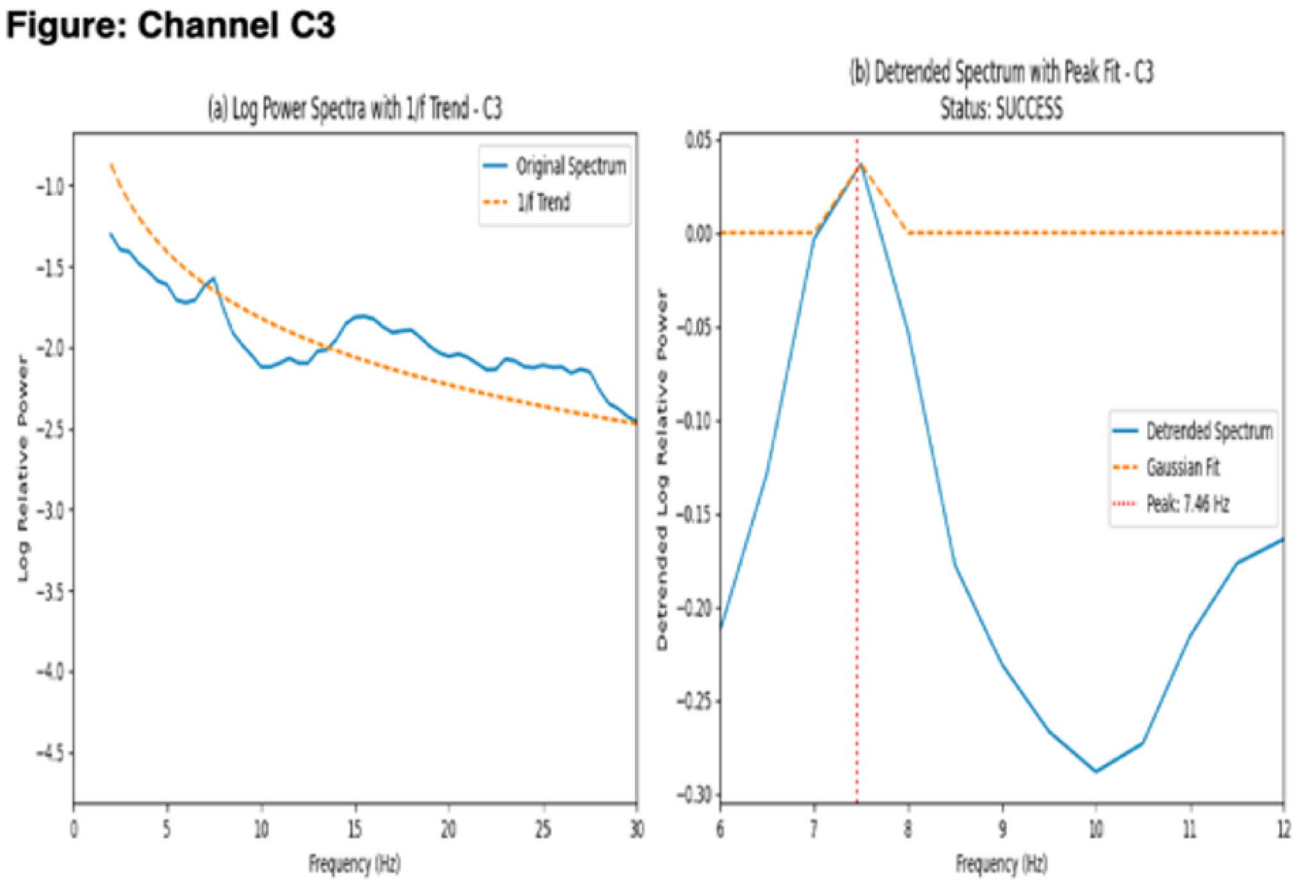

Fig. 1. Example Peak Detection.

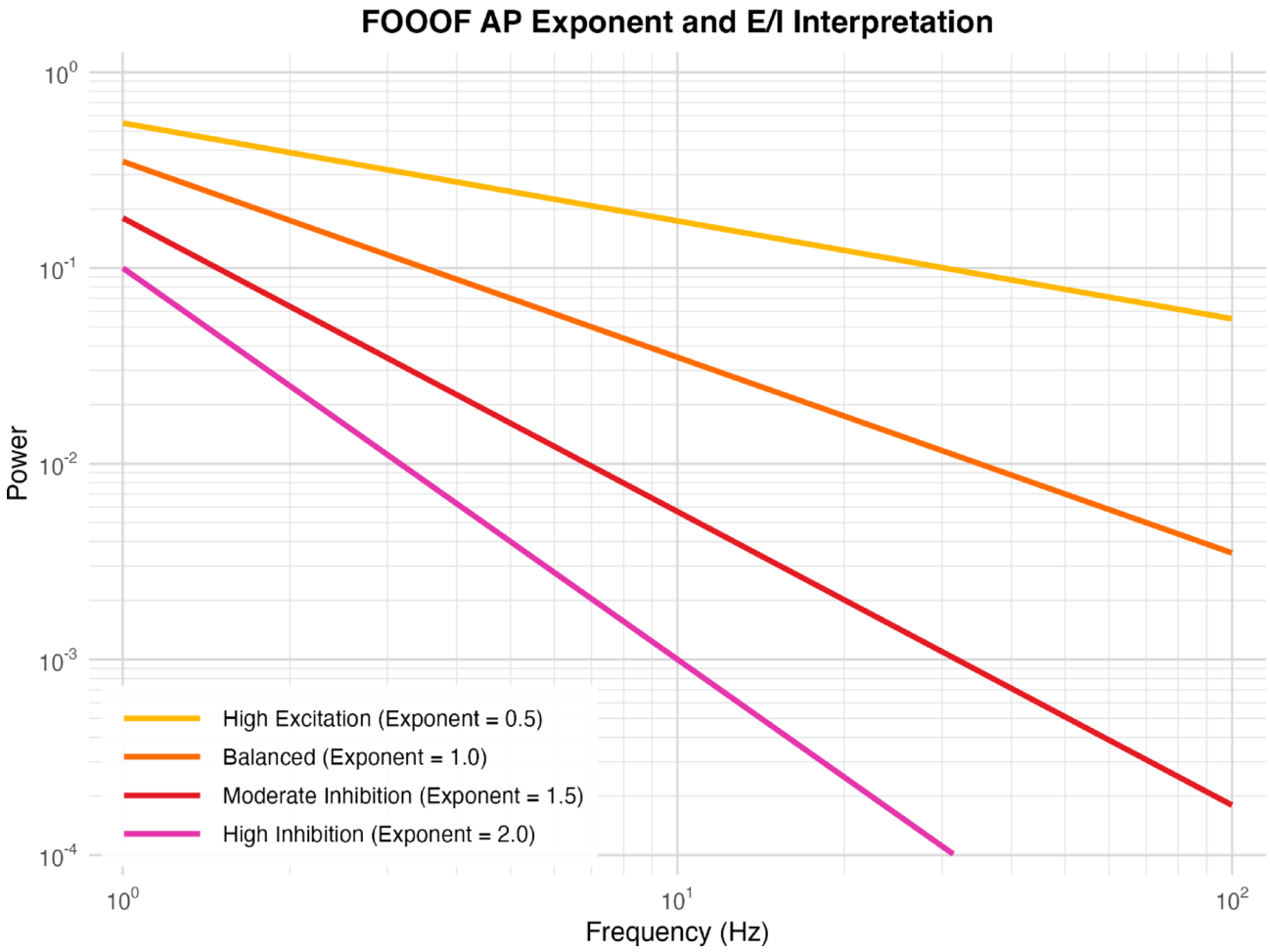

Fig. 2. Interpretation of Excitability based on FOOOF Aperiodic Slope.

frequency regions of interest (ROIs) for statistical analysis, focusing on gamma (30–71 Hz) for single trial power (STP), and multiple time-frequency windows within the 2–13 Hz range for ITC, specifically capturing onset and offset responses, as well as sustained 40 Hz and 80 Hz ITC responses to the chirp stimulus.

Statistical analysis

Analysis Populations.

The primary analysis population comprised all randomized participants who met all major eligibility criteria, received at least one dose of study medication, and completed at least one efficacy assessment (Full Analysis Population, FAP). Safety analyses included all randomized participants who received any amount of study drug (Safety Population, SP).

Statistical model specification

For all efficacy endpoints including neurophysiological, clinical, and cognitive measures, linear mixed-effects models were employed using SAS (PROC GLIMMIX, SAS 9.4; SAS Institute, Cary, NC). to assess treatment differences. The distribution of outcome variables was assessed using the Shapiro-Wilk test to verify normality assumptions ($p > 0.05$), with appropriate transformations applied when necessary to achieve normal distribution.

The mixed-effects model included fixed effects for drug treatment, drug sequence, and drug period (included to account for carry-over and period effects). Participant was modeled as a random effect (G-side), with period within participant included as an R-side random effect. Various covariance structures were examined, including first-order ante-dependence, with selection based on the lowest corrected Akaike Information Criterion. Age and IQ were considered as covariates, along with baseline assessments from the most recent assessment prior to study drug administration in treatment period 1.

Restricted maximum likelihood estimation was used with Type 3 tests of fixed effects and generalized least-squares, applying the Kenward-Roger correction to the selected covariance structure. The robust covariance matrix estimator was also considered. This approach utilized all available data from all participants to provide robust handling of data assumed missing at random.

Primary and secondary clinical endpoint analysis

For the Clinical Global Impressions-Improvement (CGI-I) scale rated by clinician and caregiver, the model included CGI-I scores collected post-dose as the outcome variable with baseline CGI-severity (CGI-S) scores as covariates. The performance-based NIH Cognitive Toolbox clinical endpoints were analyzed using change from baseline as the outcome variable with corresponding baseline scores as covariates.

For neurophysiological endpoints, EEG power spectral density analysis was performed across predefined frequency bands: delta (1–4 Hz), theta (4–8 Hz), alpha1 (8–10 Hz), alpha2 (10–12 Hz), beta (12–30 Hz), gamma1 (30–50 Hz), and gamma2 (50–70 Hz) with gamma1 power the primary EEG endpoint. A secondary neurophysiological endpoint focused on improvement in auditory intertrial phase coherence in the gamma range in response to chirp stimulus. Statistical analysis employed the same linear mixed-effects framework with treatment condition and brain region as fixed effects and participant as a random effect, accounting for the crossover design structure. Detailed EEG preprocessing and analysis methodologies are described separately in accordance with established neurophysiological analysis protocols.

Effect size and multiple comparisons

Hedges' g effect sizes were calculated to assess pairwise contrasts between drug effects for all endpoints. Least squares means differences were estimated with 95% confidence intervals. If no sequence effect was detected, the model was re-fitted without that term to estimate six pairwise differences among drug effects.

Model validation and sensitivity analyses

Model assumptions were verified using standard diagnostic procedures. If linear mixed-model assumptions were not satisfied, post-hoc analyses using generalized models or beta regression were investigated based on data suitability. Missing data were handled using the mixed-model framework's robust mechanism for data assumed missing at random.

Statistical significance was set at $\alpha = 0.05$ for primary endpoints, with trends reported for p-values between 0.05 and 0.10. All analyses were performed using SAS software with validated statistical procedures, and analysis plans were finalized prior to database lock to ensure analytical integrity.

Regulatory and ethical considerations

The study was conducted in accordance with Good Clinical Practice guidelines, the Declaration of Helsinki, and applicable regulatory requirements. The protocol and all amendments were approved by the institutional review board prior to implementation. The study was registered with ClinicalTrials.gov prior to participant enrollment (NCT06413537). The project start and end dates as logged on ClinicalTrials.gov were 2024-07-05 and 2024-12-31 respectively.

Results

Participant characteristics and study completion

Ten adult men with FXS with a mean age of 32.9 (8.27) years were enrolled (See Table 1; Fig. 3: **Consort Diagram** for additional information). Enrolled patients' medical histories were reflective of the FXS clinical phenotype with anxiety disorders highly prevalent affecting 8 participants (80%), with 5 participants receiving anxiolytic medications. Attention deficit hyperactivity disorder was present in 3 participants (30%), with 2 receiving pharmacological treatment. The presence of concomitant medications was carefully documented to assess potential interactions with study drug and ensure appropriate safety monitoring throughout the trial.

Overall primary study endpoint: safety and tolerability

SPG601 800 mg was well tolerated with a favorable safety profile. No probably or possibly treatment-related adverse effects were noted. No serious adverse events, deaths, or study discontinuations occurred. No clinically significant changes in vital signs, electrocardiographic parameters, or physical examination findings were observed. Assessment of suicidal ideation using the Columbia Suicide Severity Rating Scale revealed no instances of suicidal thoughts or behaviors throughout the study period.

Primary neurophysiological endpoints

Resting-state EEG power spectral analysis

SPG601 demonstrated significant modulation of resting-state EEG power spectral density compared to placebo across multiple frequency bands known to be disrupted in FXS (See Table 2 **for** full results).

Significant treatment effects were observed for gamma1 power ($F = 5.20$, $p = 0.023$), alpha2 power ($F = 17.43$, $p < 0.001$), and theta power ($F = 7.06$, $p = 0.008$), with directional change in each band being consistent with normalization of activity. Notably, no significant region effects or condition × region interactions were detected, indicating that treatment effects were consistent across brain regions. Power by region plots on drug versus placebo are presented for all power bands (Fig. 4). Peak alpha frequency showed no significant treatment effects ($p = 0.932$), suggesting that SPG601 modulated power within frequency bands without shifting the fundamental oscillatory frequency. These findings demonstrate selective modulation of cortical oscillatory activity following acute treatment with SPG601 with specifically directional normalization of excessive resting state gamma1 band and deficient resting state alpha2 power that characterize aberrant male FXS neurophysiology[18,26,39,40].

Aperiodic neural activity analysis

Linear mixed-effects modeling was conducted to examine SPG601 effects on the aperiodic slope of resting-state EEG power spectra, which reflects the 1/f background neural activity independent of oscillatory components and provides insights into the balance between excitatory and inhibitory neural activity. SPG601 significantly

Characteristic	All Participants ($N = 10$)
Age, years	
Mean (SD)	32.9 (8.27)
Sex, n (%)	
Male	10 (100.0)
Female	0 (0.0)
Weight, kg	
Mean (SD)	92.40 (18.164)
Height, cm	
Mean (SD)	178.32 (5.241)
BMI, kg/m^2	
Mean (SD)	28.95 (4.841)
Race, n (%)	
White	9 (90.0)
Black or African American	1 (10.0)
Ethnicity, n (%)	
Not Hispanic or Latino	10 (100.0)
Hispanic or Latino	0 (0.0)
CGG Repeats	
Mean (SD)	> 200 (all participants)
FMR1 Methylation	Complete (all participants)
Treatment Sequence, n (%)	
SPG601 → Placebo	5 (50.0)
Placebo → SPG601	5 (50.0)

Table 1. Baseline demographics and clinical characteristics. All participants adhered to study procedures and medication administration protocols. No major protocol deviations occurred that affected primary endpoint assessment. The one-week washout period was maintained for all participants (mean washout: 7.1 ± 0.8 days). No carry-over or period effects were noted in any of the analyses below.

modulated the aperiodic slope of neural activity ($F = 5.28$, $p = 0.022$, see Table 3), indicating alterations in the broadband 1/f component of the EEG power spectrum. No significant lobe effects or condition × lobe interactions were observed, suggesting consistent aperiodic changes across brain regions. The SPG601-associated aperiodic slope shift is consistent with a reduction in excessive excitatory/inhibitory balance in FXS. This finding complements the oscillatory power results and suggests that SPG601 influences both rhythmic and arrhythmic components of neural activity, potentially reflecting changes in the underlying excitation-inhibition balance in cortical circuits.

Auditory-evoked gamma oscillations

Chirp-evoked EEG measures were analyzed using linear mixed-effects models to assess treatment effects on intertrial coherence (ITC) and single trial power (STP) across gamma frequency bands. Chirp is a measure of the brain's ability to oscillate at frequencies that match the pitch or frequency of a presented auditory stimulus. None of the chirp-evoked measures showed significant treatment effects (all $p > 0.05$, see Table 4). The lack of effect on auditory-evoked responses may reflect different underlying neural mechanisms between spontaneous and stimulus-driven gamma generation, or may indicate that auditory-evoked measures require chronic dosing or higher drug concentrations to detect treatment effects.

Clinical and cognitive endpoints

No differences were noted on the Clinical Global Impressions Improvement Subscale (CGI-I) as rated by Caregiver (mean 3.7 on placebo v. 3.8 on SPG601) or Clinician (mean 3.8 on placebo v. 3.6 on SPG601). Change sensitive scores (CSS) were utilized from the NIH Toolbox 3rd Edition to evaluate potential performance-based cognitive change with treatment (See Forest Plots for all NIH TB CSS data). A significant SPG601-associated improvement was noted on the Flanker Inhibitory Control and Attention Test from the NIH TB ($p = 0.0277$; placebo: −2.6 [9.15] vs. SPG601: 3.5 [8.43]; effect size 0.85). No other individual NIH TB subtests or the Crystallized Cognition Composite index showed significant treatment associated effects. A Fluid Cognition Composite (4 subscales assessed) and Total Cognition Composite (all 6 subscales assessed) showed an SPG601-associated trend towards improved ($p = 0.0854$ and $p = 0.0843$, respectively; effects sizes 0.63 and 0.65 respectively). See Forest Plots below for individual and composite NIH TB results and Table 5 below for all confidence intervals and LS Mean Standard Deviations for drug and placebo by measure. An exploratory post-hoc subanalysis noted that no clear pattern exists suggesting that Flanker performance was driven exclusively by participants with ADHD and ADHD medication use Fig. 5.

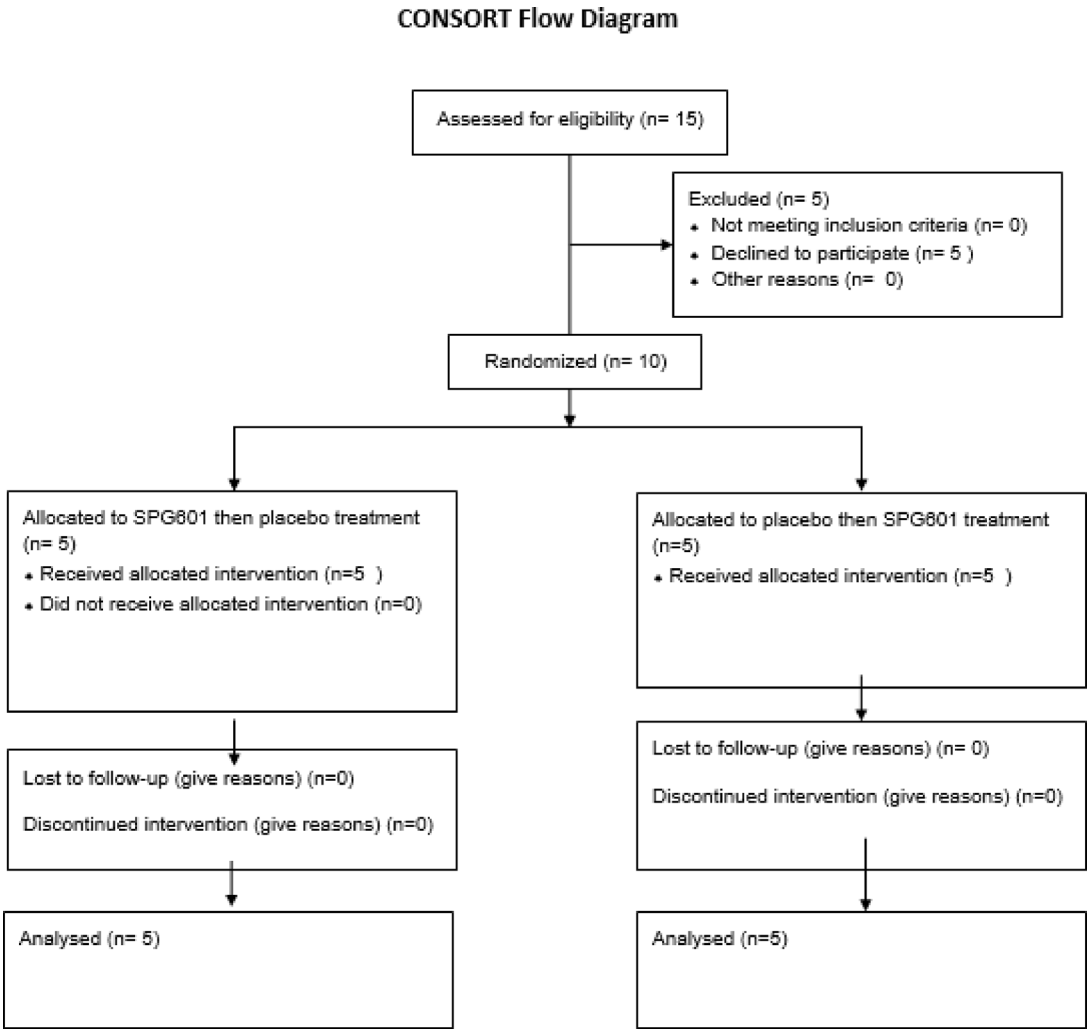

Fig. 3. Consort diagram.

Frequency band	F (df)	*p*-value	Hedges' g	95% CI	Effect Direction (SPG-601 vs. Placebo)
Alpha1 (8–10 Hz)	21.05 (1, 298)	< 0.001***	0.51	[−0.35, 1.36]	Increase
Alpha2 (10–12 Hz)	17.43 (1, 298)	< 0.001***	0.46	[−0.39, 1.31]	Increase
Theta (4–8 Hz)	7.06 (1, 298)	0.008**	0.29	[−0.55, 1.14]	Increase
Delta (1–4 Hz)	6.57 (1, 298)	0.011*	−0.28	[−1.13, 0.56]	Decrease
Gamma1 (30–50 Hz)	5.20 (1, 298)	0.023*	−0.25	[−1.10, 0.59]	Decrease
Gamma2 (50–70 Hz)	0.76 (1, 298)	0.383	−0.10	[−0.94, 0.74]	Decrease
Beta (12–30 Hz)	0.37 (1, 298)	0.544	−0.07	[−0.91, 0.77]	Decrease

Table 2. Primary EEG Endpoints: Resting-State Power Spectral Density. NumDF, numerator degrees of freedom; DenDF, denominator degrees of freedom. $p < 0.05$, $p < 0.01$, $p < 0.001$.

Fragile X messenger ribonucleoprotein levels

Pharmacodynamic assessment of FMRP levels was successfully completed in 8 of 10 participants, with 2 additional participants having historical FMRP data from prior studies included with appropriate consent. FMRP levels confirmed the characteristic protein deficiency expected in full-mutation fragile X syndrome.

FMRP was detectable in 5 participants at levels ≤ 1.7 picomoles, with 5 participants showing undetectable levels (0 picomoles) (See Table 6). These levels are substantially below those typically observed in unaffected individuals (20–40 picomoles), confirming the characteristic protein deficiency in the study population[37].

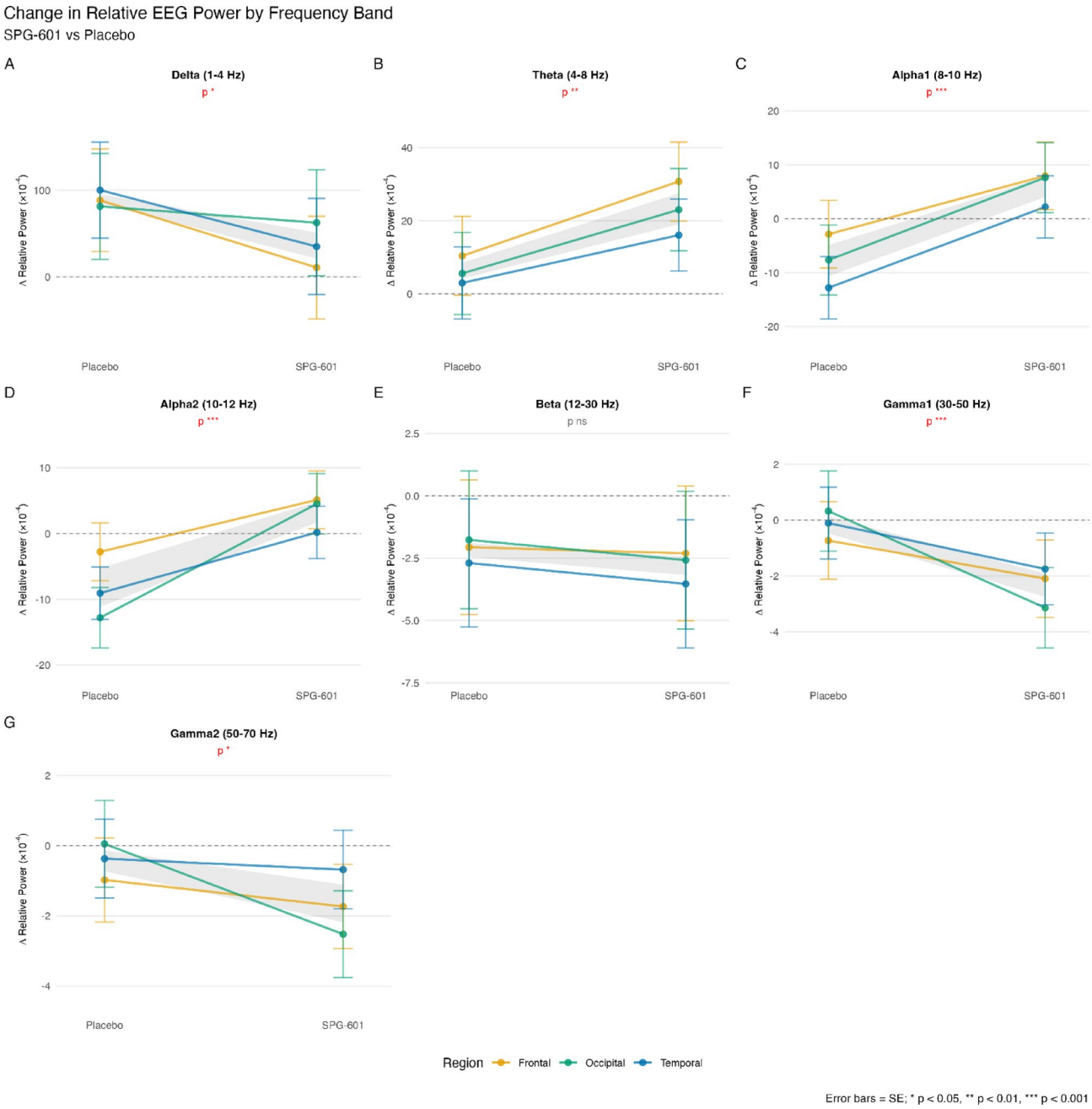

Fig. 4. All power bands change in EEG resting power by brain region by treatment condition.

Variable	Sum Sq	Mean Sq	NumDF	DenDF	F value	*p*-value
Condition	0.36171	0.36171	1	587	5.2844	0.022*
Lobe	0.01846	0.01846	1	587	0.2697	0.604
Condition × Lobe	0.00571	0.00571	1	587	0.0835	0.773

Table 3. Aperiodic Slope Analysis. Sum Sq, sum of squares; Mean Sq, mean squares; NumDF, numerator degrees of freedom; DenDF, denominator degrees of freedom. *$p < 0.05$.

Discussion

The results obtained in this study represent the first time a drug treatment in FXS has rescued well established resting EEG abnormalities while also showing significant performance-based outcome measure improvement. The demonstration of robust EEG biomarker responses across multiple neurophysiological domains, coupled

Measure	Estimate	Std Error	F-statistic	DF	*p*-value
ITC 40 Hz	0.00315	0.0127	0.249	16	0.807
ITC 80 Hz	−0.00490	0.0176	−0.279	16	0.784
STP Gamma1	0.282	0.586	0.481	16	0.637
SA Ratio	4.43	5.11	0.867	16	0.399
ITC Onset Latency	−0.0351	0.0244	−1.44	16	0.170

Table 4. Chirp-Evoked EEG measures. ITC, intertrial coherence; STP, single trial power; SA, synchronization-asynchronization; DF, degrees of freedom.

Paradigm	95% CI for LS Means	Mean Change from Baseline (SD) Placebo vs. SPG601	*p*-value
Flanker Inhibitory Control and Attention Test	−12.39, 0.1438	−2.6 (9.15) vs. 3.5 (8.43)	0.0277
Dimensional Change Card Sort Test	-17.03, 5.029	-5.3 (17.20) vs0.7 (12.89)	0.1432
Pattern Comparison Processing Speed Test	−18.19, 7.936	8.4 (12.07) 13.5 (26.05)	0.2209
Picture Vocabulary Test	−3.33, 7.552	0.6 (3.40) vs. −1.6 (7.49)	0.2235
Oral Symbol Digit Test	−15.54, 8.539	3.3 (11.30) vs. 6.8 (11.51)	0.2844
Oral Reading Recognition	−1.701, 3.847	−3.1 (9.13) vs. −4.1 (8.86)	0.2241
Crystallized Cognition Composite	−3.674, 10.77	−2.4 (10.53) vs. −5.7 (2.81)	0.1678
Fluid Cognition Composite	−56.27, 9.979	6.0 (30.40) vs. 29.1 (44.18)	0.0854
Total Cognition Composite	−57.76, 10.1	4.7 (31.42) vs. 22.0 (47.05)	0.0843

Table 5. NIH Toolbox Paradigm Change Sensitive Scores Summary Statistics.

with specific improvements in executive function and a favorable safety profile, establishes proof-of-concept for SPG601 as a therapeutic strategy in FXS and further validates the translational utility of comprehensive electrophysiological endpoints in this population[17,18,26,28,39–49].

The observed pattern of EEG changes following SPG601 administration provides compelling evidence for comprehensive neurophysiological target engagement. This is the first time that a pharmacotherapy in FXS has been associated with improvement, or an increase, in alpha2 band power (10–12 Hz). This finding aligns with emerging evidence that alpha oscillations serve as critical gating mechanisms for attention and cognitive control, with increased alpha2 power associated with enhanced selective attention and reduced distractibility[50,51]. The enhancement of alpha2 power suggests restoration of thalamocortical regulatory mechanisms that are fundamentally disrupted in FXS, consistent with the pulvinar-cortical interaction model where alpha oscillations modulate neuronal gain in thalamo-cortical circuits[51].

The concurrent modulation of gamma (30–70 Hz) and theta (4–8 Hz) band power provides additional mechanistic insight into the specific impact of BK channel activity with SPG601. Excessive gamma1 oscillations, which were significantly reduced following SPG601 treatment ($F = 5.20$, $p = 0.023$), reflect the pathological neocortical hyperexcitability that characterizes FXS (Wang et al., 2017). This normalization aligns with preclinical observations that BK channel activation reduces epileptiform activity and excessive glutamate release in Fmr1 knockout mice[12,52]. The significant theta band modulation ($F = 7.06$, $p = 0.008$) suggests restoration of thalamocortical dynamics critical for cognitive processing, as theta oscillations coordinate information flow between cortical and subcortical structures. The broad EEG effects across frequency bands and aperiodic slope may be best interpreted as acute normalization of circuit excitability and E/I balance in FXS. This supports the broader perspective that targeting circuit-level dynamics as opposed to solely targeting upstream molecular abnormalities may be a promising therapeutic strategy in FXS and potentially other NDDs. Our results overall connect normalization of circuit dynamics with measurable, performance-based improvement in executive function.

In addition to significant benefits in resting EEG parameters relevant to FXS, SPG601 treatment was found to modulate aperiodic EEG activity. This is the first demonstration of such for a pharmacotherapy in FXS, or in any form of developmental disability. The aperiodic EEG slope measure provides critical insight into the balance between excitatory and inhibitory neural activity and has emerged as increasingly relevant in neurodevelopmental disorders[53]. The demonstration that SPG601 affects both rhythmic and arrhythmic components of neural activity suggests that BK channel activation influences fundamental aspects of cortical circuit dynamics, potentially reflecting changes in the underlying excitation-inhibition balance. This finding is particularly significant given emerging evidence that aperiodic EEG exponents reflect developmental processes and may serve as sensitive markers of neural circuit maturation[54]. We believe that normalization of rhythmic and arrhythmic neural activity in FXS may positively impact sensory processing, sensory hypersensitivities,

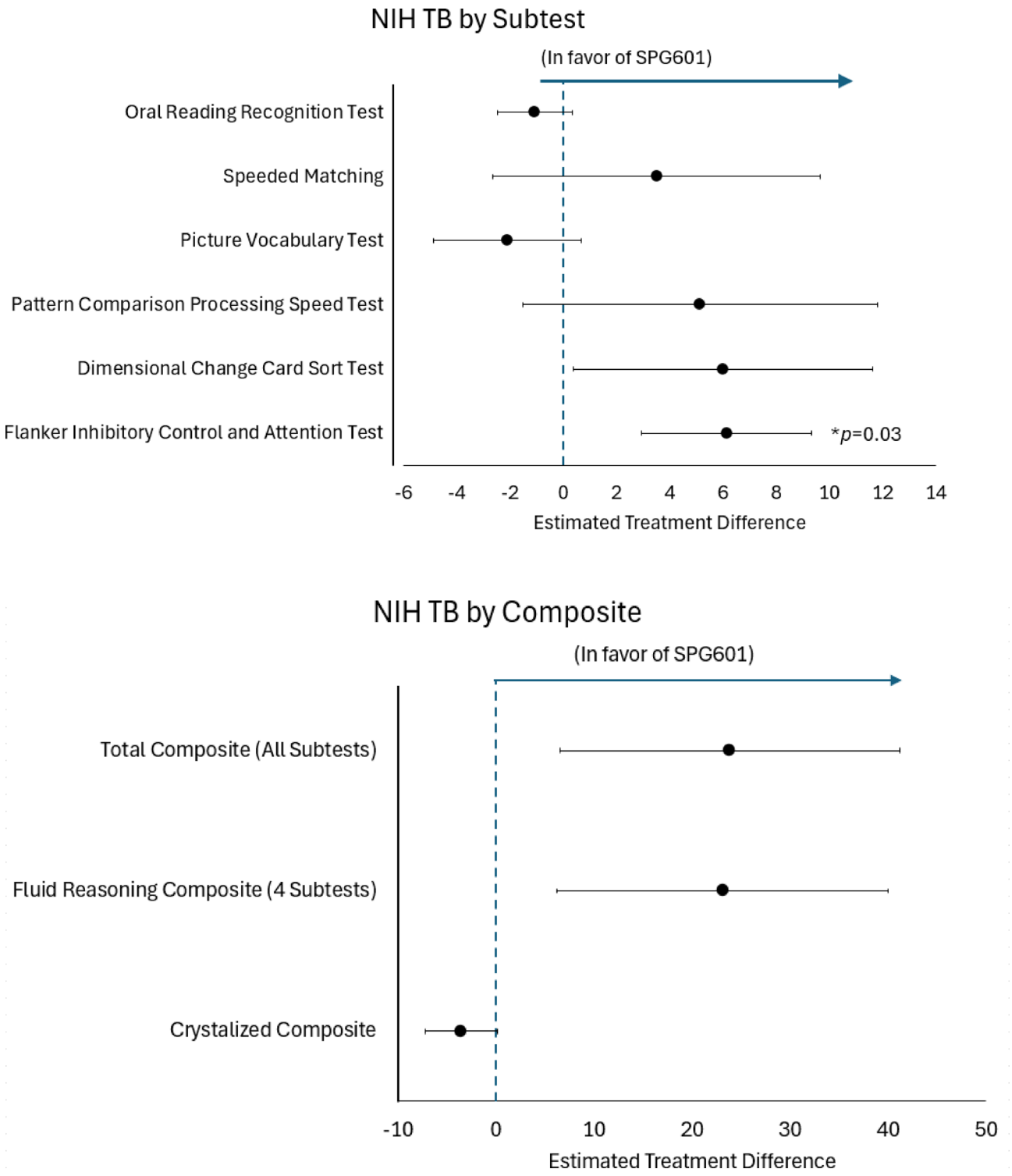

Fig. 5. NIH Toolbox Forest Plots.

and interfering anxiety along other symptoms that clinically characterize FXS and at baseline correlate with the degree of neurophysiologic impairment as measured by EEG[39,40].

On a behavioral level, SPG601 treatment was associated with a significant improvement in the NIH TB Flanker task. This is of particular importance given the FXS-specific nature of Flanker deficits and the fact that no prior candidate therapy has been shown to improve performance on this attentional measure. NIH TB Flanker has been demonstrated to have higher reliability and lower overall scores in FXS than in populations with Down Syndrome (DS) or other intellectual disability[36,55], highlighting a uniquely severe deficit in attention as a core disability in FXS. Additionally, Dimensional Change Card Sort is another executive function test

Participant ID	FMRP Level (picomoles)
101-001	0.33
101-002	0
101-003	0
101-004	0.84
101-005	0.20
101-006	1.70
101-007	0
101-008	0.23
101-009	0
101 – 010	0

Table 6. Individual Participant FMRP Levels.

element within NIH TB that, like Flanker, shows differentiation in FXS from other forms of NDD with FXS being associated with more significant impairment[36,55]. In our report, SPG601 treatment was associated with a similar numeric improvement in DCCS as Flanker, but our DCCS data had more variability and thus did not make a $p < 0.05$ threshold.

Across-species study in FXS suggests that suppression of distraction is deficient in both the FMR1 KO mouse and in humans with FXS[56]. Overall, Flanker and DCCS represent executive function tests whose results in FXS are consistent with the well-established specific executive function impairment that characterizes FXS[36]. Interestingly, DCCS and Flanker are the only two NIH Toolbox subscales whose scores in FXS have demonstrated significant association with FXS molecular genetic measures, with higher scores associated with increasing FMR1 mRNA expression in FXS[57]. No other NIH Toolbox measures have demonstrated a significant relationship with the molecular genetic deficit that defines FXS.

The concurrent enhancement of alpha 2 power and Flanker performance provides convergent neurophysiological and behavioral evidence for improved thalamocortical function. This relationship is consistent with emerging theoretical frameworks proposing that pulvinar-mediated alpha oscillations serve as priority maps for attention, orchestrating the synchrony of cortico-cortical interactions to render neural communication more effective and selective[51]. The temporal correlation between electrophysiological normalization and cognitive improvement following SPG601 dosing supports a mechanistic link between BK channel activation, circuit restoration, and functional outcomes. We believe continued functional, performance-based improvement over time may lead to improvement in activities of daily living including communication and learning.

Several study limitations must be acknowledged. The single-dose design, while appropriate for proof-of-concept evaluation, limits conclusions about chronic efficacy and optimal dosing strategies. The small sample size ($n = 10$), though consistent with early-phase neuropharmacology studies, may limit generalizability and effect size precision. The acute single dose nature of the treatment may make it difficult to infer chronic functional outcomes associated with repeated dosing. While there may be practice or placebo learning effects on cognitive tests in a crossover design, we did not note period or carryover effects in our analysis. While we did not find that ADHD comorbidity status or medication use by drug class impacted the study results when modeling for these factors, given the small sample we cannot confirm or deny that either specific concomitant medication use by drug class or comorbid diagnosis/diagnoses may in some way impact future study results. It will be essential to conduct pre-specified sub-analyses in future larger trials to evaluate the impact of potential comorbid diagnoses and/or concomitant medication use of treatment response. The restriction to adult males limits applicability to females and pediatric populations where greater neuroplasticity might enhance therapeutic benefit. At the same time, this approach enables focus small first in FXS target engagement study on specific neurophysiologic dysregulation well established specifically in males with FXS. The crossover design, while statistically efficient, required careful consideration of potential carryover effects. The absence of sequence effects in statistical analyses and the rapid elimination kinetics of SPG601 support minimal carryover influence, though future chronic studies may consider parallel-group design. In this first in FXS pilot study, we did not employ rigorous correction for multiple comparisons such as Bonferroni correction. While this may be appropriate for small hypothesis generating trials that inform future well power investigations, this approach does introduce risk of Type I error in results interpretation. The absence of significant changes in global clinical measures (CGI-I scales) likely reflects both the single-dose design and the limited sensitivity of these instruments to acute pharmacological effects. The comprehensive neurophysiological and cognitive assessment battery proved more sensitive to treatment effects, supporting their use as primary endpoints in future studies.

The demonstration of neurophysiological target engagement and selective cognitive improvement provides strong rationale for advancing SPG601 to chronic dosing studies. The effect sizes observed for EEG and NIH TB endpoints suggest clinically meaningful biological activity that may translate to meaningful functional improvements with sustained treatment. The favorable safety profile supports dose escalation studies to optimize therapeutic benefit while maintaining the observed safety margin.

Conclusions

This study provides the first clinical evidence that SPG601 represents a viable and promising therapeutic strategy for fragile X syndrome. The demonstration of comprehensive neurophysiological changes across multiple

domains, coupled with selective cognitive improvements in executive function, establishes robust proof-of-concept for this novel mechanism. This work justifies exploring chronic dosing trials in adults and potential future additional studies in youth with FXS where plasticity may be greater. The validation of EEG biomarkers as sensitive measures of target engagement addresses a critical need in neurodevelopmental disorder clinical trials and may accelerate therapeutic development.

These findings represent a potential breakthrough in addressing the significant unmet medical need in this specific neurodevelopmental disorder and may inform therapeutic approaches for other genetic conditions characterized by ion channel dysfunction and circuit hyperexcitability. The mechanistic insights gained from this study advance our understanding of FXS pathophysiology and provide a foundation for precision medicine approaches in neurodevelopmental disorders.

Data availability

The data that support the findings of this study are available from Spinogenix. Restrictions apply to the availability of these data, which were used under license for this study. Data are available with the permission of Spinogenix.

Received: 8 September 2025; Accepted: 28 March 2026
Published online: 07 April 2026

References

1. van der Lei, M. B. & Kooy, R. F. From Discovery to Innovative Translational Approaches in 80 Years of Fragile X Syndrome Research. *Biomedicines* **13** (4), 805 (2025).
2. Hagerman, R. J. et al. Fragile X syndrome. *Nat. Rev. Dis. Primers*. **3**, 17065 (2017).
3. Budimirovic, D. B. & Protic, D. D. Fragile X syndrome: Recent research updates toward capturing treatments' improvement in clinical trials. *Brain Sci.* **12** (10), 1276 (2022).
4. Darnell, J. C. et al. FMRP Stalls Ribosomal Translocation on mRNAs Linked to Synaptic Function and Autism. *Cell* **146**, 247–261 (2011).
5. Berry-Kravis, E. Mechanism-based treatments in neurodevelopmental disorders: fragile X syndrome. *Pediatr. Neurol.* **50** (4), 297–302 (2014).
6. Kshatri, A. et al. Differential regulation of BK channels by fragile X mental retardation protein. *J. Gen. Physiol.* **152** (6), 1–17 (2020).
7. Short, B. FMRP differentially regulates BK channels. *J. Gen. Physiol.* **152** (6), 1–17 e202012634 (2020).
8. Hurley, M. J. et al. Reversal of behavioural phenotype by the cannabinoid-like compound VSN16R in fragile X syndrome mice. *Brain* **145** (1), 76–82 (2022).
9. Zhan, X. et al. Calcium-Dependent Regulation of Neuronal Excitability Is Rescued in Fragile X Syndrome by a Tat-Conjugated N-Terminal Fragment of FMRP. *J. Neurosci.* **44** (21), 1–14 e0136242024 (2024).
10. Liao, L. et al. Quantitative proteomic analysis of primary neurons reveals diverse changes in synaptic protein content in fmr1 knockout mice. *Proc. Natl. Acad. Sci. U S A*. **105**, 15281–15286 (2008).
11. Laumonnier, F. et al. Association of a functional deficit of the BKCa channel, a synaptic regulator of neuronal excitability, with autism and mental retardation. *Am. J. Psychiatry*. **163**, 1622–1629 (2006).
12. Deng, P. Y. et al. FMRP regulates neurotransmitter release and synaptic information transmission by modulating action potential duration via BK channels. *Neuron* **77** (4), 696–711 (2013).
13. Deng, P. Y. & Klyachko, V. A. Genetic upregulation of BK channel activity normalizes multiple synaptic and circuit defects in a mouse model of fragile X syndrome. *J. Physiol.* **594** (1), 83–97 (2016).
14. Myrick, L. K. et al. Independent role for presynaptic FMRP revealed by an FMR1 missense mutation associated with intellectual disability and seizures. *Proc. Natl. Acad. Sci. U S A*. **112** (4), 949–956 (2015).
15. Griguoli, M., Sgritta, M. & Cherubini, E. Presynaptic BK channels control transmitter release: physiological relevance and potential therapeutic implications. *J. Physiol.* **594** (13), 3489–3500 (2016).
16. Hebert, B. et al. Rescue of fragile X syndrome phenotypes in Fmr1 KO mice by a BKCa channel opener molecule. *Orphanet J. Rare Dis.* **9**, 124 (2014).
17. Ethridge, L. E. et al. Neural synchronization deficits linked to cortical hyper-excitability and auditory hypersensitivity in fragile X syndrome. *Mol. Autism*. **8**, 22 (2017).
18. Wang, J. et al. A resting EEG study of neocortical hyperexcitability and altered functional connectivity in fragile X syndrome. *J. Neurodev Disord*. **9**, 11 (2017).
19. Martire, M. et al. Pre-synaptic BK channels selectively control glutamate versus GABA release from cortical and hippocampal nerve terminals. *J. Neurochem*. **115** (2), 411–422 (2010).
20. Kimm, T., Khaliq, Z. M. & Bean, B. P. Differential Regulation of Action Potential Shape and Burst-Frequency Firing by BK and Kv2 Channels in Substantia Nigra Dopaminergic Neurons. *J. Neurosci.* **35** (50), 16404–16417 (2015).
21. Nisar, S. et al. Genetics of glutamate and its receptors in autism spectrum disorder. *Mol. Psychiatry*. **27** (5), 2380–2392 (2022).
22. Mitchell, D. E. et al. Altered integration of excitatory inputs onto the basal dendrites of layer 5 pyramidal neurons in a mouse model of Fragile X syndrome. *Proc. Natl. Acad. Sci. U S A*. **120** (2), e2208963120 (2023).
23. Carreno-Munoz, M. I. et al. Potential Involvement of Impaired BK(Ca) Channel Function in Sensory Defensiveness and Some Behavioral Disturbances Induced by Unfamiliar Environment in a Mouse Model of Fragile X Syndrome. *Neuropsychopharmacology* **43** (3), 492–502 (2018).
24. Zhang, Y. et al. Dendritic channelopathies contribute to neocortical and sensory hyperexcitability in Fmr1(-/y) mice. *Nat. Neurosci.* **17** (12), 1701–1709 (2014).
25. Pedapati, E. V. et al. Neocortical localization and thalamocortical modulation of neuronal hyperexcitability contribute to Fragile X Syndrome. *Commun. Biol.* **5** (1), 442 (2022).
26. Ethridge, L. E. et al. Validating brain activity measures as reliable indicators of individual diagnostic group and genetically mediated sub-group membership Fragile X Syndrome. *Sci. Rep.* **14** (1), 22982 (2024).
27. Takarae, Y. et al. EEG Microstates as Markers for Cognitive Impairments in Fragile X Syndrome. *Brain Topogr*. **37** (3), 432–446 (2024).
28. Liu, R. et al. Reliability of resting-state electrophysiology in fragile X syndrome. *Biomark. Neuropsychiatry* **9** 1–19. (2023).
29. Berry-Kravis, E. M. et al. Inhibition of phosphodiesterase-4D in adults with fragile X syndrome: a randomized, placebo-controlled, phase 2 clinical trial. *Nat. Med.* **27** (5), 862–870 (2021).
30. Janz, P. et al. Clinically-probed mechanisms of action in Fragile-X syndrome fail to normalize translational EEG phenotypes in Fmr1 knockout mice. *Neuropharmacology* **262**, 110182 (2025).

31. Tabatabaee, S. et al. The Cannabinoid-Like Compound, VSN16R, Acts on Large Conductance, Ca(2+)-Activated K(+) Channels to Modulate Hippocampal CA1 Pyramidal Neuron Firing. *Pharmaceuticals (Basel)* **12** (3), 1–12 (2019).
32. Baker, D. et al. Big conductance calcium-activated potassium channel openers control spasticity without sedation. *Br. J. Pharmacol.* **174** (16), 2662–2681 (2017).
33. Pryce, G. et al. Neuroprotection in an Experimental Model of Multiple Sclerosis via Opening of Big Conductance, Calcium-Activated Potassium Channels. *Pharmaceuticals (Basel)* **16** (7), 1–13 (2023).
34. Kenny, A., Wright, D. & Stanfield, A. C. EEG as a translational biomarker and outcome measure in fragile X syndrome. *Translational Psychiatry*. **12** (1), 35 (2022).
35. Wilkinson, C. L. & Nelson, C. A. Increased aperiodic gamma power in young boys with Fragile X Syndrome is associated with better language ability. *Mol. Autism*. **12**, 17 (2021).
36. Shields, R. H. et al. Validation of the NIH Toolbox Cognitive Battery in intellectual disability. *Neurology*, e1229–e1240 (2020).
37. Boggs, A. E. et al. Optimization, validation and initial clinical implications of a Luminex-based immunoassay for the quantification of Fragile X Protein from dried blood spots. *Sci. Rep.* **12** (1), 5617 (2022).
38. Dickinson, A. et al. Peak alpha frequency is a neural marker of cognitive function across the autism spectrum. *Eur. J. Neurosci.* **47** (6), 643–651 (2018).
39. Smith, E. G. et al. Sex differences in resting EEG power in Fragile X Syndrome. *J. Psychiatr Res.* **138**, 89–95 (2021).
40. Pedapati, E. V. et al. Frontal cortex hyperactivation and gamma desynchrony in Fragile X syndrome: Correlates of auditory hypersensitivity. *PLoS One*. **20** (5), e0306157 (2025).
41. Van der Molen, M. J. & Van der Molen, M. W. Reduced alpha and exaggerated theta power during the resting-state EEG in fragile X syndrome. *Biol. Psychol.* **92** (2), 216–219 (2013).
42. van der Molen, M. J. W., Stam, C. J. & van der Molen, M. W. Resting-State EEG Oscillatory Dynamics in Fragile X Syndrome: Abnormal Functional Connectivity and Brain Network Organization. *PLoS ONE*. **9** (2), e88451 (2014).
43. Lovelace, J. W. et al. Translation-relevant EEG phenotypes in a mouse model of Fragile X Syndrome. *Neurobiol. Dis.* **115**, 39–48 (2018).
44. Ethridge, L. E. et al. Auditory EEG Biomarkers in Fragile X Syndrome: Clinical Relevance. *Front. Integr. Neurosci.* **13**, 60 (2019).
45. Goswami, S. et al. Local cortical circuit correlates of altered EEG in the mouse model of Fragile X syndrome. *Neurobiol. Dis.* **124**, 563–572 (2019).
46. Jonak, C. R. et al. Multielectrode array analysis of EEG biomarkers in a mouse model of Fragile X Syndrome. *Neurobiol. Dis.* **138**, 104794 (2020).
47. Razak, K. A., Binder, D. K. & Ethell, I. M. Neural Correlates of Auditory Hypersensitivity in Fragile X Syndrome. *Front. Psychiatry*. **12**, 720752 (2021).
48. Jonak, C. R. et al. Baclofen-associated neurophysiologic target engagement across species in fragile X syndrome. *J. Neurodev Disord*. **14** (1), 52 (2022).
49. Jonak, C. R. et al. Phenotypic analysis of multielectrode array EEG biomarkers in developing and adult male Fmr1 KO mice. *Neurobiol. Dis.* **195**, 106496 (2024).
50. Weiss, S. M. & Marshall, P. J. Anticipation across modalities in children and adults: Relating anticipatory alpha rhythm lateralization, reaction time, and executive function. *Dev. Sci.* **26** (1), e13277 (2023).
51. Bourgeois, A. et al. Pulvino-cortical interaction: An integrative role in the control of attention. *Neurosci. Biobehav. Rev.* **111**, 104–113 (2020).
52. Ferraguto, C. et al. Therapeutic efficacy of the BKCa channel opener chlorzoxazone in a mouse model of Fragile X syndrome. *Neuropsychopharmacology* **49** (13), 2093–2104 (2024).
53. Carter Leno, V. et al. Infant excitation/inhibition balance interacts with executive attention to predict autistic traits in childhood. *Mol. Autism*. **13**, 52 (2022).
54. Stanyard, R. A. et al. Aperiodic and Hurst EEG exponents across early human brain development: A systematic review. *Dev. Cogn. Neurosci.* **68**, 101402 (2024).
55. Shields, R. H. et al. Sensitivity of the NIH Toolbox to Detect Cognitive Change in Individuals With Intellectual and Developmental Disability. *Neurology* **100** (8), e778–e789 (2023).
56. Rahmatullah, N. et al. Hypersensitivity to Distractors in Fragile X Syndrome from Loss of Modulation of Cortical VIP Interneurons. *J. Neurosci.* **43** (48), 8172–8188 (2023).
57. Aishworiya, R. et al. Intercorrelation of Molecular Biomarkers and Clinical Phenotype Measures in Fragile X Syndrome. *Cells*, **12** (14), 1–16 (2023).

Author contributions

All authors reviewed and edited the manuscript. SS, PV, SG, EVP, and CAE conceptualized the experiments. CAE, PV, and EVP wrote the main manuscript text. EVP and CAE prepared all manuscript Tables and Figures. GW participated in data acquisition, data processing and analysis. SR and MN participated in data acquisition and analysis.

Funding

The work described in this manuscript was funded by Spinogenix Inc.

Declarations

Competing interests

The work was funded by Spinogenix.

Additional information

Supplementary Information The online version contains supplementary material available at https://doi.org/10.1038/s41598-026-46928-6.

Correspondence and requests for materials should be addressed to C.A.E.